AIMS Mathematics, 10(3): 6144–6167.
DOI: 10.3934/math.2025280
Received: 20 January 2025
Revised: 02 March 2025
Accepted: 05 March 2025
Published: 19 March 2025

https://www.aimspress.com/journal/Math

Research article

Numerical solution of forward and inverse problems of heat conduction in multi-layered media

Yu Xu[1], Youjun Deng[1,*] and Dong Wei[2]

[1] School of Mathematics and Statistics, Central South University, Changsha, Hunan 410083, China
[2] China Aerodynamics Research and Development Center, Mianyang, Sichuan 621000, China

*** Correspondence:** Emai: youjundeng@csu.edu.cn.

Abstract: The primary objective of this paper was to delve into the exploration of numerical methods for solving forward and inverse problems related to heat conduction in one-dimensional multi-layered media. To address the non-differentiability at multilayer medium interfaces that prevents direct discretization, this paper employed the finite volume method to construct finite difference schemes. Compared with traditional difference methods, the proposed method improved accuracy by considering coefficient variations near interfaces. For the ill-posed initial value problem in inverse heat conduction of multilayer media, we transformed the inverse problem into an operator equation using the finite volume method for forward problems. The Landweber iterative regularization method combined with the Morozov discrepancy principle was then applied to obtain iterative sequences. Numerical simulations demonstrate the algorithm's superior accuracy and noise resistance compared with conventional methods through comparative studies and sensitivity analyses.

Keywords: heat conduction; multi-layered media; forward and inverse problems; finite difference method; iterative regularization
Mathematics Subject Classification: 65M08, 65M32

1. Introduction

The issue of heat conduction in multi-layered media has garnered significant attention in both industrial applications and scientific research, emerging as a crucial and challenging area of study.

This is evident in various contexts such as heat transfer dynamics of multi-layer protective clothing [1], temperature fluctuations within wellbores and geological formations comprised of multiple layers [2], and the insulation properties of multi-layered materials used in low-temperature containers [3]. These real-world examples underscore the complexity and practical relevance of accurately modeling heat conduction in multi-layered media. The mathematical analysis of multi-layered media has also undergone a noteworthy breakthrough (i.e., [3–9]).

Ever since Lessem proposed the problem of heat conduction for porous media in 1957, extensive research has been conducted by scholars on this particular issue [10]. In 1951, Landweber proposed the Landweber iterative regularization method for solving linear problems [11]. In 1967, Tikhonov proposed the Tikhonov variational regularization method based on the principle of variation [12], providing substantial means for solving heat conduction inversion problems. In 1987, Elden investigated the sideways parabolic equations in multi-layered media [13,14]. Huang studied the conjugate gradient method to solve the three-dimensional transient inverse heat conduction problem in 1999 [15]. In 2009, Connors J proposed partitioned time stepping for a parabolic two domain problem [16]. In 2019, Shi developed a finite analytical method for heat transfer in heterogeneous media [17]. In 2022, Wang presented a theoretical study on the optimization of key material parameters of multilayer clothing assemblies [18]. In 2023, Wu proposed a homogenization model for modeling 3D heterogeneous porous elastic media [19,20]. Recently, Hou proposed a stable state–based ring dynamic heat transfer model to investigate the interfacial thermal resistance of materials with complex heat transfer constitutive relations [21,22]. At the same time, Wu proposed a homogenization model based on the numerical manifold method for nonlinear transient heat conduction in heterogeneous media [23,24]. The numerical manifold method has high computational accuracy and is suitable for complex interface conditions, showing great potential. However, it requires a large amount of computation compared with the finite volume method, and the noise resistance when applied to inversion is still to be verified.

In practical problems, the multi-layered medium heat conduction problem cannot be solved analytically, and the calculation volume may escalate significantly as the number of layers increases. The traditional difference schemes usually replace the coefficient of the interface with the arithmetic average or harmonic average of the coefficient near the interface; however, they ignore the variation of the coefficient near the interface in heterogeneous media and fail to fully ensure the continuity of heat flux. Traditional numerical methods also present difficulties in solving the inverse problem of heat conduction in multi-layered media. In this paper, we will mainly provide numerical solution methods for the forward and inverse problems of multi-layered non-uniform medium heat conduction and verify the effectiveness and feasibility of the algorithms. The structure of this paper is organized as follows: In Section 3, we present our finite volume method–based difference scheme for the forward problem of heat conduction in multi-layered media. Also, we apply the forward problem's difference scheme to construct the operator equation for the inverse heat conduction problem in multi-layered media. Then, we solve this equation using the Landweber iterative regularization method. In Section 4, we demonstrate the accuracy and effectiveness of our methods through numerical simulations. The conclusions are given in Section 5.

This method avoids direct discretization of the interface. Instead, it constructs the scheme by using the integrability of differential equations and continuity conditions of heat flux. Thus, the method overcomes the limitation of traditional difference methods in handling non-differentiable interfaces, takes coefficient variations into account, and ensures more accurate continuity of heat flux.

Numerical experiments demonstrate that this method achieves higher accuracy while maintaining computational efficiency compared to traditional difference methods.

2. Heat conduction equations in multi-layered media

Consider the one-dimensional multi-layer heat conduction equation in a medium, where the spatial axis is x, the time variable is t, and the time interval is $[0,T]$. In a rod composed of multiple layers of medium, let $0 = x^0 < x^1 < \mathrm{L} < x^{n-1} < x^n = l$, where the length of the rod is l, and the interval of the i-th layer of medium is $\left[x^{i-1}, x^i\right]$, $i = 1,2,\mathrm{L}\ ,n$, as shown in Figure 1.

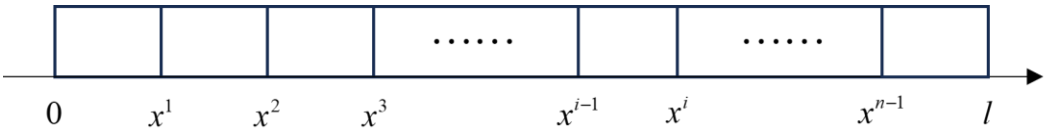

Figure 1. Schematic diagram of multi-layered medium heat conduction.

Let the temperature function of the rod be $u(x,t)$, where the initial temperature at time $t = 0$ is $f(x)$, the boundary temperature at $x = 0$ is $\alpha(t)$, and the boundary temperature at $x = l$ is $\beta(t)$. Let us assume that the physical parameters in the medium are only dependent on spatial parameters x and are continuous functions. Let the temperature function, thermal conductivity, density, and specific heat capacity of the i-th layer of the medium be denoted by $u^i(x,t)$, $k^i(x)$, $\rho^i(x)$, and $c^i(x)$, respectively. Let the heat source intensity of the medium be $q^i(x,t)$. Using the first law of thermodynamics and Fourier's law, the temperature function $u^i(x,t)$ satisfies the following equation:

$$\begin{cases} c^i(x)\rho^i(x)\dfrac{\partial u^i}{\partial t} = \dfrac{\partial}{\partial x}\left(k^i(x)\dfrac{\partial u^i}{\partial x}\right) + q^i(x,t), x^{i-1} < x < x^i \\ u(x,0) = f(x) \\ u(0,t) = \alpha(t) \\ u(l,t) = \beta(t) \\ 0 < x < l, 0 < t < T \end{cases} \quad ,i = 1,2,\mathrm{L}\ ,n, \tag{2.1}$$

At the interface between media, there are the following connection conditions:

$$\begin{cases} u^i\big|_{x=x^i} = u^{i+1}\big|_{x=x^i} \\ -k^{i+1}\dfrac{\partial u}{\partial x}^{i+1}\Big|_{x=x^i} = -k^i\dfrac{\partial u}{\partial x}^{i}\Big|_{x=x^i} \end{cases} \quad ,0 \le t \le T, i = 1,2,\mathrm{L}\ ,n-1. \tag{2.2}$$

3. Forward and inverse problems in multi-layered medium heat conduction

3.1. Numerical solution of the forward problem

Consider Eqs (2.1) and (2.2) as follows:

$$\begin{cases} c^i(x)\rho^i(x)\dfrac{\partial u^i}{\partial t} = \dfrac{\partial}{\partial x}\left(k^i(x)\dfrac{\partial u^i}{\partial x}\right) + q^i(x,t), x^{i-1} < x < x^i \\ u(x,0) = f(x) \\ u(0,t) = \alpha(t) \\ u(l,t) = \beta(t) \\ 0 < x < l, 0 < t < T \end{cases}, i = 1,2,\mathrm{L}\ ,n,$$

and

$$\begin{cases} u^i\big|_{x=x^i} = u^{i+1}\big|_{x=x^i} \\ -k^{i+1}\dfrac{\partial u}{\partial x}^{i+1}\Big|_{x=x^i} = -k^i\dfrac{\partial u}{\partial x}^{i}\Big|_{x=x^i} \end{cases}, 0 \le t \le T, i = 1,2,\mathrm{L}\ ,n-1,$$

where $c^i(x), \rho^i(x), k^i(x)$ are continuous functions on $\left(x^{i-1}, x^i\right)$. We now solve for the temperature function $u(x,t)$.

For the interior of the i-th medium, the spatial interval $\left[x^{i-1}, x^i\right]$ is uniformly divided into a total of J^i parts, and the nodes are denoted as $x^{i-1} = x_0^i < x_1^i < \mathrm{L} < x_{J^i-1}^i < x_{J^i}^i = x^i$, with the space-step size $h^i = \dfrac{x^{i-1} - x^i}{J^i}$. The approximate value of $u^i(x,t)$ at node $x = x_j^i$ is taken as $u_j^i(t)$, and the spatial interval s is then dual-meshed, with the nodes denoted as $x^i_{j-\frac{1}{2}} = \dfrac{x_j^i + x_{j-1}^i}{2}$.

Use the finite volume method to construct a difference scheme: for $x = x_j, j = 1,2,\mathrm{L}\ ,J^i - 1$, the first equation in (2.1) is integrated over the interval $\left[x^i_{j-\frac{1}{2}}, x^i_{j+\frac{1}{2}}\right]$ to give the following:

$$\int_{x^i_{j-\frac{1}{2}}}^{x^i_{j+\frac{1}{2}}} c^i(x)\rho^i(x)\frac{\partial u^i}{\partial t}dx = k^i(x)\frac{\partial u^i}{\partial x}\Big|_{x^i_{j-\frac{1}{2}}}^{x^i_{j+\frac{1}{2}}} + \int_{x^i_{j-\frac{1}{2}}}^{x^i_{j+\frac{1}{2}}} q^i(x,t)dx, \tag{3.1}$$

Let us denote $c^i\left(x_j^i\right), \rho^i\left(x_j^i\right), k^i\left(x_j^i\right)$ as c_j^i, ρ_j^i, k_j^i and use the rectangle formula to obtain the following:

$$h^i c_j^i \rho_j^i \frac{\partial u_j^i}{\partial t} = k^i_{j+\frac{1}{2}}\frac{u_{j+1}^i(t) - u_j^i(t)}{h^i} - k^i_{j-\frac{1}{2}}\frac{u_j^i(t) - u_{j-1}^i(t)}{h^i} + \int_{x^i_{j-\frac{1}{2}}}^{x^i_{j+\frac{1}{2}}} q^i dx, \tag{3.2}$$

Divide the time interval $[0,T]$ into K parts and let $0=t_0<t_1<\mathrm{L}<t_{K-1}<t_K=T$ be the time node, $\tau_k=t_k-t_{k-1}$ the time-step size, and $u_{j,k}^i$ the approximate value of the function $u^i(x,t)$ at the node (x_j^i,t_k). Denote $q_{j,k}^i=\frac{1}{h^i}\int_{x_{j-\frac{1}{2}}^i}^{x_{j+\frac{1}{2}}^i}q^i(x,t_k)dx$. Use the trapezoidal rule and discretize the time variable as follows:

$$\begin{aligned}&h^ic_j^i\rho_j^i\frac{u_{j,k+1}^i-u_{j,k}^i}{\tau_{k+1}}\\&=\theta\left(k_{j+\frac{1}{2}}^i\frac{u_{j+1,k+1}^i-u_{j,k+1}^i}{h^i}-k_{j-\frac{1}{2}}^i\frac{u_{j,k+1}^i-u_{j-1,k+1}^i}{h^i}+h^iq_{j,k+1}^i\right),\\&+(1-\theta)\left(k_{j+\frac{1}{2}}^i\frac{u_{j+1,k}^i-u_{j,k}^i}{h^i}-k_{j-\frac{1}{2}}^i\frac{u_{j,k}^i-u_{j-1,k}^i}{h^i}+h^iq_{j,k}^i\right)\end{aligned}\tag{3.3}$$

where $\theta\in[0,1]$.

For the interface between media, let u_k^i be the approximate value of the function $u^i(x,t)$ at the node (x^i,t_k). Denote $q_{j^i,k}^i=\frac{2}{h^i}\int_{x_{j^i-\frac{1}{2}}^i}^{x_{j^i}^i}q^i(x,t_k)dx$, $q_{0,k}^{i+1}=\frac{2}{h^{i+1}}\int_{x_0^{i+1}}^{x_{\frac{1}{2}}^i}q^{i+1}(x,t_k)dx$. The finite volume method and the connection condition (2.2) can be used to obtain

$$\begin{aligned}&\frac{h^ic_{j^i}^i\rho_{j^i}^i+h^{i+1}c_0^{i+1}\rho_0^{i+1}}{2}\frac{u_{k+1}^i-u_k^i}{\tau_{k+1}}\\&=\theta\left(k_{\frac{1}{2}}^{i+1}\frac{u_{1,k+1}^{i+1}-u_{k+1}^i}{h^{i+1}}-k_{j^i-\frac{1}{2}}^i\frac{u_{k+1}^i-u_{j^i-1,k+1}^i}{h^i}+\frac{h^i}{2}q_{j^i,k+1}^i+\frac{h^{i+1}}{2}q_{0,k+1}^{i+1}\right),\\&+(1-\theta)\left(k_{\frac{1}{2}}^{i+1}\frac{u_{1,k}^{i+1}-u_k^i}{h^{i+1}}-k_{j^i-\frac{1}{2}}^i\frac{u_k^i-u_{j^i-1,k}^i}{h^i}+\frac{h^i}{2}q_{j^i,k}^i+\frac{h^{i+1}}{2}q_{0,k}^{i+1}\right)\end{aligned}\tag{3.4}$$

We can transform (3.3) and (3.4) to obtain difference schemes:

$$\begin{aligned}&-\frac{\theta k_{j+\frac{1}{2}}^i}{h^i}u_{j+1,k+1}^i+\left(\frac{h^ic_j^i\rho_j^i}{\tau_{k+1}}+\frac{\theta k_{j-\frac{1}{2}}^i}{h^i}+\frac{\theta k_{j+\frac{1}{2}}^i}{h^i}\right)u_{j,k+1}^i-\frac{\theta k_{j-\frac{1}{2}}^i}{h^i}u_{j,k+1}^i=\\&\frac{(1-\theta)k_{j+\frac{1}{2}}^i}{h^i}u_{j+1,k}^i+\left(\frac{h^ic_j^i\rho_j^i}{\tau_{k+1}}-\frac{(1-\theta)k_{j-\frac{1}{2}}^i}{h^i}-\frac{(1-\theta)k_{j+\frac{1}{2}}^i}{h^i}\right)u_{j,k}^i+\frac{(1-\theta)k_{j-\frac{1}{2}}^i}{h^i}u_{j,k}^i,\\&+(1-\theta)h^iq_{j,k}^i+\theta h^iq_{j,k+1}^i\end{aligned}\tag{3.5}$$

and

$$
\begin{aligned}
&-\frac{\theta k_{\frac{1}{2}}^{i+1}}{h^{i+1}}u_{1,k+1}^{i+1}+\left(\frac{h^i c_{J^i}^i \rho_{J^i}^i+h^{i+1}c_0^{i+1}\rho_0^{i+1}}{2\tau_{k+1}}+\frac{\theta k_{J^i-\frac{1}{2}}^i}{h^i}+\frac{\theta k_{\frac{1}{2}}^{i+1}}{h^{i+1}}\right)u_{k+1}^i-\frac{\theta k_{J^i-\frac{1}{2}}^i}{h^i}u_{J^i-1,k+1}^i\\
&=\frac{(1-\theta)k_{\frac{1}{2}}^{i+1}}{h^{i+1}}u_{1,k}^{i+1}+\left(\frac{h^i c_{J^i}^i \rho_{J^i}^i+h^{i+1}c_0^{i+1}\rho_0^{i+1}}{2\tau_{k+1}}-\frac{(1-\theta)k_{\frac{1}{2}}^{i+1}}{h^{i+1}}-\frac{(1-\theta)k_{J^i-\frac{1}{2}}^i}{h^i}\right)u_k^i \qquad , \qquad (3.6)\\
&+\frac{(1-\theta)k_{J^i-\frac{1}{2}}^i}{h^i}u_{J^i-1,k}^i+\frac{(1-\theta)h^i}{2}q_{J^i,k}^i+\frac{(1-\theta)h^{i+1}}{2}q_{0,k}^{i+1}+\theta\frac{h^i}{2}q_{J^i,k+1}^i+\theta\frac{h^{i+1}}{2}q_{0,k+1}^{i+1}
\end{aligned}
$$

Note $U_k=\left[u_{1,k}^1,u_{2,k}^1,\mathrm{L}\ ,u_{J^1-1,k}^1,u_k^1,u_{1,k}^2,\mathrm{L}\ ,u_{J^n-1,k}^n\right]$, $J=\sum_{i=1}^{n}J^i-1$ and transform (3.5) and (3.6) into the following form:

$$AU_{k+1}=BU_k+C_k, \qquad (3.7)$$

where A, B is the $J\times J$ matrix, and C is the $J\times 1$ vector.

For the initial conditions and boundary conditions in (2.1), we have

$$
\begin{cases}
u_{j,0}^i=f\left(x_j^i\right)\\
u_{0,k}^1=\alpha\left(t_k\right)\\
u_{J^n,k}^n=\beta\left(t_k\right)
\end{cases}, \qquad (3.8)
$$

By iteratively applying (3.7) and (3.8) in time layer $k=0,1,\mathrm{L}\ ,K-1$, we can obtain $u_{j,k}^i$.

Theorem 3.1. When $\theta\in\left[0,\frac{1}{2}\right)\mathrm{U}\left(\frac{1}{2},1\right]$, the local truncation error of (3.5) is $O\left(\left(h^i\right)^2+\tau\right)$, and the local truncation error of (3.6) is $O\left(h^i+h^{i+1}+\tau\right)$. When $\theta=\frac{1}{2}$, the local truncation error of (3.5) is $O\left(\left(h^i\right)^2+\tau^2\right)$, and the local truncation error of (3.6) is $O\left(h^i+h^{i+1}+\tau^2\right)$.

Proof. Let us first consider the local truncation error of (3.5), and by using Taylor expansion on u with respect to x, we can obtain

$$
\begin{aligned}
&c_j^i\rho_j^i\frac{u_{j,k+1}^i-u_{j,k}^i}{\tau_{k+1}}\\
&=\frac{\theta}{h}\left[\left(k^i\frac{\partial u^i}{\partial x}\right)_{j+\frac{1}{2},k+1}-\left(k^i\frac{\partial u^i}{\partial x}\right)_{j-\frac{1}{2},k+1}\right]-\frac{1-\theta}{h}\left[\left(k^i\frac{\partial u^i}{\partial x}\right)_{j+\frac{1}{2},k}-\left(k^i\frac{\partial u^i}{\partial x}\right)_{j-\frac{1}{2},k}\right], \qquad (3.9)\\
&+(1-\theta)q_{j,k}^i+\theta q_{j,k+1}^i+O\left(\left(h^i\right)^2\right)
\end{aligned}
$$

Using Taylor's expansion on $k\frac{\partial u}{\partial x}$ with respect to x gives:

$$\begin{aligned} & h^i c_j^i \rho_j^i \frac{u_{j,k+1}^i - u_{j,k}^i}{\tau_{k+1}} \\ & = \frac{1}{2}\left[\theta\partial\left(k^i \frac{\partial u^i}{\partial x}\right)_{j,k+1} + (1-\theta)\partial\left(k^i \frac{\partial u^i}{\partial x}\right)_{j,k}\right] + (1-\theta) q_{j,k}^i + \theta q_{j,k+1}^i + O\left(\left(h^i\right)^2\right) \end{aligned}, \tag{3.10}$$

Using Taylor's expansion on u, $\frac{\partial}{\partial x}\left(k\frac{\partial u}{\partial x}\right)$, q with respect to t, we can obtain

$$\begin{aligned} \left(c^i \rho^i \frac{\partial u^i}{\partial t}\right)_{j,k+\frac{1}{2}} &= \frac{\partial}{\partial x}\left(k^i \frac{\partial u^i}{\partial x}\right)_{j,k+\frac{1}{2}} + q^i{}_{j,k+\frac{1}{2}} \\ &+ \frac{1-2\theta}{2}\tau\left[\frac{\partial}{\partial t \partial x}\left(k^i \frac{\partial u^i}{\partial x}\right)_{j,k+\frac{1}{2}} + \left(\frac{\partial q^i}{\partial t}\right)_{j,k+\frac{1}{2}}\right] + O\left(\left(h^i\right)^2\right) + O\left(\tau^2\right) \end{aligned}, \tag{3.11}$$

Considering the differential equation within the medium, we have

$$c^i \rho^i \left.\frac{\partial u^i}{\partial t}\right|_{j,k+\frac{1}{2}} = \left.\frac{\partial}{\partial x}\left(k^i \frac{\partial u^i}{\partial x}\right)\right|_{j,k+\frac{1}{2}} + q^i\big|_{j,k+\frac{1}{2}}, \tag{3.12}$$

Compare (3.12) with (3.11) to obtain the local truncation error of the difference scheme (3.5) when $\theta \in \left[0, \frac{1}{2}\right) \cup \left(\frac{1}{2}, 1\right]$:

$$R_{j,k+1}^i = O\left(\tau + \left(h^i\right)^2\right). \tag{3.13}$$

And when $\theta = \frac{1}{2}$, the local truncation error is:

$$R_{j,k+1}^i = O\left(\tau^2 + \left(h^i\right)^2\right). \tag{3.14}$$

Then, consider the local truncation error of (3.6), and by using Taylor expansion on u with respect to x, we can obtain

$$\begin{aligned} & \frac{h^i c_{J^i}^i \rho_{J^i}^i + h^{i+1} c_0^{i+1} \rho_0^{i+1}}{2} \frac{u_{k+1}^i - u_k^i}{\tau_{k+1}} \\ & = \theta\left[\left(k^{i+1}\frac{\partial u^{i+1}}{\partial x}\right)_{\frac{1}{2},k+1} - \left(k^i \frac{\partial u^i}{\partial x}\right)_{J^i-\frac{1}{2},k+1}\right] + (1-\theta)\left[\left(k^{i+1}\frac{\partial u^{i+1}}{\partial x}\right)_{\frac{1}{2},k+1} - \left(k^i \frac{\partial u^i}{\partial x}\right)_{J^i-\frac{1}{2},k+1}\right], \\ & + \frac{\theta}{2}\left(\frac{h^i}{2} q_{J^i,k+1}^i + \frac{h^{i+1}}{2} q_{0,k+1}^{i+1}\right) + \frac{1-\theta}{2}\left(\frac{h^i}{2} q_{J^i,k}^i + \frac{h^{i+1}}{2} q_{0,k}^{i+1}\right) + O\left(\left(h^i\right)^3 + \left(h^{i+1}\right)^3\right) \end{aligned} \tag{3.15}$$

Using Taylor's expansion on $k\dfrac{\partial u}{\partial x}$ with respect to x gives:

$$\begin{aligned}
&\frac{h^i c_{J^i}^i \rho_{J^i}^i + h^{i+1} c_0^{i+1} \rho_0^{i+1}}{2} \frac{u_{k+1}^i - u_k^i}{\tau_{k+1}} \\
&= \frac{\theta}{2}\left[h^{i+1} \frac{\partial}{\partial x}\left(k^{i+1} \frac{\partial u^{i+1}}{\partial x} \right)_{0,k+1} + h^i \frac{\partial}{\partial x}\left(k^i \frac{\partial u^i}{\partial x} \right)_{J^i,k+1} \right] \\
&+ \frac{1-\theta}{2}\left[h^{i+1} \frac{\partial}{\partial x}\left(k^{i+1} \frac{\partial u^{i+1}}{\partial x} \right)_{0,k} + h^i \frac{\partial}{\partial x}\left(k^i \frac{\partial u^i}{\partial x} \right)_{J^i,k} \right] \\
&+ \frac{\theta}{6}\left[\left(h^{i+1}\right)^2 \frac{\partial^2}{\partial x^2}\left(k^{i+1} \frac{\partial u^{i+1}}{\partial x} \right)_{0,k+1} - \left(h^i\right)^2 \frac{\partial^2}{\partial x^2}\left(k^i \frac{\partial u^i}{\partial x} \right)_{J^i,k+1} \right] \\
&+ \frac{1-\theta}{6}\left[\left(h^{i+1}\right)^2 \frac{\partial^2}{\partial x^2}\left(k^{i+1} \frac{\partial u^{i+1}}{\partial x} \right)_{0,k} - \left(h^i\right)^2 \frac{\partial^2}{\partial x^2}\left(k^i \frac{\partial u^i}{\partial x} \right)_{J^i,k} \right] \\
&+ \frac{\theta}{2}\left(\frac{h^i}{2} q_{J^i,k+1}^i + \frac{h^{i+1}}{2} q_{0,k+1}^{i+1} \right) + \frac{1-\theta}{2}\left(\frac{h^i}{2} q_{J^i,k}^i + \frac{h^{i+1}}{2} q_{0,k}^{i+1} \right) + O\left(\left(h^i\right)^3 + \left(h^{i+1}\right)^3 \right)
\end{aligned}, \tag{3.16}$$

Using Taylor's expansion on u, $\dfrac{\partial}{\partial x}\left(k\dfrac{\partial u}{\partial x} \right)$, q with respect to t, we can obtain

$$\begin{aligned}
&h^i \left(c^i \rho^i \frac{\partial u^i}{\partial t} \right)_{J^i,k+\frac{1}{2}} + h^{i+1} \left(c^{i+1} \rho^{i+1} \frac{\partial u^{i+1}}{\partial t} \right)_{0,k+\frac{1}{2}} = h^{i+1} \frac{\partial}{\partial x}\left(k^{i+1} \frac{\partial u^{i+1}}{\partial x} \right)_{0,k+\frac{1}{2}} + h^i \frac{\partial}{\partial x}\left(k^i \frac{\partial u^i}{\partial x} \right)_{J^i,k+\frac{1}{2}} \\
&+ \left(h^i q_{J^i,k+\frac{1}{2}}^i + h^{i+1} q_{0,k+\frac{1}{2}}^{i+1} \right) + \frac{\theta}{3}\left[\left(h^{i+1}\right)^2 \frac{\partial^2}{\partial x^2}\left(k^{i+1} \frac{\partial u^{i+1}}{\partial x} \right)_{0,k+1} - \left(h^i\right)^2 \frac{\partial^2}{\partial x^2}\left(k^i \frac{\partial u^i}{\partial x} \right)_{J^i,k+1} \right] \\
&+ \frac{1-\theta}{3}\left[\left(h^{i+1}\right)^2 \frac{\partial^2}{\partial x^2}\left(k^{i+1} \frac{\partial u^{i+1}}{\partial x} \right)_{0,k} - \left(h^i\right)^2 \frac{\partial^2}{\partial x^2}\left(k^i \frac{\partial u^i}{\partial x} \right)_{J^i,k} \right] \\
&+ \frac{1-2\theta}{2}\tau \left[h^{i+1} \left(\frac{\partial}{\partial t \partial x}\left(k^{i+1} \frac{\partial u^{i+1}}{\partial x} \right) + \frac{\partial q^{i+1}}{\partial t} \right)_{0,k+\frac{1}{2}} + h^i \left(\frac{\partial}{\partial t \partial x}\left(k^i \frac{\partial u^i}{\partial x} \right) + \frac{\partial q^i}{\partial t} \right)_{J^i,k+\frac{1}{2}} \right] \\
&+ O\left(\left(h^i\right)^3 + \left(h^{i+1}\right)^3 + \left(h^i + h^{i+1}\right)\tau^2 \right)
\end{aligned}, \tag{3.17}$$

Considering the differential equation at the interface between media, we have

$$\begin{aligned}
&\frac{h^i}{h^i + h^{i+1}} \left(c^i \rho^i \frac{\partial u^i}{\partial t} \right)_{J^i,k+\frac{1}{2}} + \frac{h^{i+1}}{h^i + h^{i+1}} \left(c^{i+1} \rho^{i+1} \frac{\partial u^{i+1}}{\partial t} \right)_{0,k+\frac{1}{2}} \\
&= \frac{h^i}{h^i + h^{i+1}} \frac{\partial}{\partial x}\left(k^i \frac{\partial u^i}{\partial x} \right)_{J^i,k+\frac{1}{2}} + \frac{h^{i+1}}{h^i + h^{i+1}} \frac{\partial}{\partial x}\left(k^{i+1} \frac{\partial u^{i+1}}{\partial x} \right)_{0,k+\frac{1}{2}} + \frac{h^i}{h^i + h^{i+1}} q_{J^i,k+\frac{1}{2}}^i + \frac{h^{i+1}}{h^i + h^{i+1}} q_{0,k+\frac{1}{2}}^{i+1}
\end{aligned}, \tag{3.18}$$

Compare (3.17) with (3.18) to obtain the local truncation error of the difference scheme (3.5) when $\theta \in \left[0,\frac{1}{2}\right)\mathrm{U}\left(\frac{1}{2},1\right]$:

$$R_{k+1}^{i}=O\left(h^{i}+h^{i+1}+\tau\right), \tag{3.19}$$

And when $\theta=\frac{1}{2}$, the local truncation error is:

$$R_{k+1}^{i}=O\left(h^{i}+h^{i+1}+\tau^{2}\right), \tag{3.20}$$

Therefore, Theorem 3.1 is proved. □

Theorem 3.2. When $\theta \in \left[\frac{1}{2},1\right]$, the difference schemes (3.5) and (3.6) satisfy stability conditions.

Proof. Using the freezing coefficient method, we freeze the variable coefficients k_j^i, k_j^{i+1} into constant coefficients k^i, k^{i+1}, rewrite the variable coefficient formulas (3.5) and (3.6) into their corresponding constant coefficient difference schemes, and then use the Fourier method to substitute $u_{j,k}^{i}=v_k e^{ijh}$ and $u_k^i=u_{J^i,k}^i=v_k e^{iaJ^ih}$ to obtain:

$$\begin{aligned}
&-\frac{\theta k^i}{h^i}v_{k+1}e^{ia(j+1)h}+\left(\frac{h^ic_j^i\rho_j^i}{\tau_{k+1}}+\frac{2\theta k^i}{h^i}\right)v_{k+1}e^{iajh}-\frac{\theta k_j^i}{h^i}v_{k+1}e^{ia(j-1)h}=\\
&\frac{(1-\theta)k^i}{h^i}v_k e^{ia(j+1)h}+\left(\frac{h^ic_j^i\rho_j^i}{\tau_{k+1}}-\frac{2(1-\theta)k^i}{h^i}\right)v_k e^{iajh}+\frac{(1-\theta)k^i}{h^i}v_k e^{ia(j-1)h},\\
&+(1-\theta)h^iq_{j,k}^i+\theta h^iq_{j,k+1}^i
\end{aligned} \tag{3.21}$$

and

$$\begin{aligned}
&-\frac{\theta k^{i+1}}{h^{i+1}}v_{k+1}e^{ia(J^i+1)h}+\left(\frac{h^ic_{J^i}^i\rho_{J^i}^i+h^{i+1}c_0^{i+1}\rho_0^{i+1}}{2\tau_{k+1}}+\frac{\theta k^i}{h^i}+\frac{\theta k^{i+1}}{h^{i+1}}\right)v_{k+1}e^{iaJ^ih}-\frac{\theta k^i}{h^i}v_{k+1}e^{ia(J^i-1)h}\\
&=\frac{(1-\theta)k^{i+1}}{h^{i+1}}v_k e^{ia(J^i+1)h}+\left(\frac{h^ic_{J^i}^i\rho_{J^i}^i+h^{i+1}c_0^{i+1}\rho_0^{i+1}}{2\tau_{k+1}}-\frac{(1-\theta)k^{i+1}}{h^{i+1}}-\frac{(1-\theta)k^i}{h^i}\right)v_k e^{iaJ^ih}\\
&+\frac{(1-\theta)k^i}{h^i}v_k e^{ia(J^i-1)h}+\frac{(1-\theta)h^i}{2}q_{J^i,k}^i+\frac{(1-\theta)h^{i+1}}{2}q_{0,k}^{i+1}+\theta\frac{h^i}{2}q_{J^i,k+1}^i+\theta\frac{h^{i+1}}{2}q_{0,k+1}^{i+1}
\end{aligned}, \tag{3.22}$$

The growth factor is:

$$G_1(ph,\tau)=\frac{c_j^i\rho_j^i-2(1-\theta)\frac{\tau_{k+1}}{(h^i)^2}k^i(1-\cos\alpha h)}{c_j^i\rho_j^i+2\theta\frac{\tau_{k+1}}{(h^i)^2}k^i(1-\cos\alpha h)}, \tag{3.23}$$

And

$$G_2(ph,\tau)=\frac{\frac{h^i c_{j^i}^i \rho_{j^i}^i + h^{i+1} c_0^{i+1} \rho_0^{i+1}}{2\tau_{k+1}} - (1-\theta)\left(\frac{k^{i+1}}{h^{i+1}}+\frac{k^i}{h^i}\right)(1-\cos\alpha h) + i(1-\theta)\left(\frac{k^{i+1}}{h^{i+1}}-\frac{k^i}{h^i}\right)\sin\alpha h}{\frac{h^i c_{j^i}^i \rho_{j^i}^i + h^{i+1} c_0^{i+1} \rho_0^{i+1}}{2\tau_{k+1}} + \theta\left(\frac{k^{i+1}}{h^{i+1}}+\frac{k^i}{h^i}\right)(1-\cos\alpha h) - i\theta\left(\frac{k^{i+1}}{h^{i+1}}-\frac{k^i}{h^i}\right)\sin\alpha h}, \quad (3.24)$$

Obviously, when $\theta\in\left[\frac{1}{2},1\right]$, we always have:

$$\left|G_1(ph,\tau)\right|\le 1, \quad (3.25)$$

and

$$\left|G_2(ph,\tau)\right|\le 1, \quad (3.26)$$

Therefore, the difference schemes (3.5) and (3.6) are proved to be stable.□

However, the schemes may become unstable when $\theta\in\left(0,\frac{1}{2}\right)$, but we can stabilize them by restricting the mesh ratio.

Theorem 3.3. When $\theta\in\left(0,\frac{1}{2}\right)$, if the maximum mesh ratio $r=\max\frac{\tau_k}{\left(h^i\right)^2}$ always has $r\le\frac{c^i(x)\rho^i(x)}{2(1-2\theta)k^i(x)}$, the difference schemes (3.5) and (3.6) satisfy stability conditions.

Proof. When $\theta\in\left(0,\frac{1}{2}\right)$, if $r\le\frac{c^i(x)\rho^i(x)}{2(1-2\theta)k^i(x)}$, obviously, we always have:

$$\left|G_1(ph,\tau)\right|\le 1. \quad (3.27)$$

We only need to prove $\left|G_2(ph,\tau)\right|\le 1$, namely

$$\begin{aligned}&\left(\frac{h^i c_{j^i}^i \rho_{j^i}^i + h^{i+1} c_0^{i+1} \rho_0^{i+1}}{2\tau_{k+1}} - (1-\theta)\left(\frac{k^{i+1}}{h^{i+1}}+\frac{k^i}{h^i}\right)(1-\cos\alpha h)\right)^2 + \left((1-\theta)\left(\frac{k^{i+1}}{h^{i+1}}-\frac{k^i}{h^i}\right)\sin\alpha h\right)^2 \\ &\le\left(\frac{h^i c_{j^i}^i \rho_{j^i}^i + h^{i+1} c_0^{i+1} \rho_0^{i+1}}{2\tau_{k+1}} + \theta\left(\frac{k^{i+1}}{h^{i+1}}+\frac{k^i}{h^i}\right)(1-\cos\alpha h)\right)^2 + \left(\theta\left(\frac{k^{i+1}}{h^{i+1}}-\frac{k^i}{h^i}\right)\sin\alpha h\right)^2\end{aligned}, \quad (3.28)$$

It is equivalent to prove

$$\frac{h^i c_{j^i}^i \rho_{j^i}^i + h^{i+1} c_0^{i+1} \rho_0^{i+1}}{\tau_{k+1}}\left(\frac{k^{i+1}}{h^{i+1}}+\frac{k^i}{h^i}\right) - 2(1-2\theta)\left(\left(\frac{k^{i+1}}{h^{i+1}}\right)^2+\left(\frac{k^i}{h^i}\right)^2 - 2\left(\frac{k^{i+1}}{h^{i+1}}+\frac{k^i}{h^i}\right)\cos\alpha h\right)\ge 0, \quad (3.29)$$

And we have

$$\begin{aligned}
&\frac{h^i c^i_{J^i}\rho^i_{J^i}+h^{i+1}c_0^{i+1}\rho_0^{i+1}}{\tau_{k+1}}\left(\frac{k^{i+1}}{h^{i+1}}+\frac{k^i}{h^i}\right)-2(1-2\theta)\left(\left(\frac{k^{i+1}}{h^{i+1}}\right)^2+\left(\frac{k^i}{h^i}\right)^2-2\left(\frac{k^{i+1}}{h^{i+1}}+\frac{k^i}{h^i}\right)\cos\alpha h\right)\\
&\geq\frac{h^i c^i_{J^i}\rho^i_{J^i}+h^{i+1}c_0^{i+1}\rho_0^{i+1}}{\tau_{k+1}}\left(\frac{k^{i+1}}{h^{i+1}}+\frac{k^i}{h^i}\right)-2(1-2\theta)\left(\frac{k^{i+1}}{h^{i+1}}+\frac{k^i}{h^i}\right)^2 \qquad , (3.30)\\
&=\left(\frac{k^{i+1}}{h^{i+1}}+\frac{k^i}{h^i}\right)\left(\left(\frac{(h^i)^2}{\tau_{k+1}}-\frac{2(1-2\theta)k^i}{c^i_{J^i}\rho^i_{J^i}}\right)\frac{k^i c^i_{J^i}\rho^i_{J^i}}{h^i}+\left(\frac{(h^{i+1})^2}{\tau_{k+1}}-\frac{2(1-2\theta)k^{i+1}}{c_0^{i+1}\rho_0^{i+1}}\right)\frac{k^{i+1}c_0^{i+1}\rho_0^{i+1}}{h^{i+1}}\right)\geq 0
\end{aligned}$$

Therefore, $\left|G_2(ph,\tau)\right|\leq 1$.

It implies that the difference schemes (3.5) and (3.6) are stable.□

When $\theta\in\left(0,\frac{1}{2}\right)$, the stability condition can be optimized by decreasing the time step τ_k or increasing the space step h^i. Because of its unconditional stability and higher convergence order, $\theta=\frac{1}{2}$ is usually taken in calculations.

3.2. Numerical solution of the forward problem

Consider equations (2.1) and (2.2) as follows:

$$\begin{cases}
c^i(x)\rho^i(x)\dfrac{\partial u^i}{\partial t}=\dfrac{\partial}{\partial x}\left(k^i(x)\dfrac{\partial u^i}{\partial x}\right)+q^i(x),\ x^{i-1}<x<x^i\\
u(x,0)=f(x)\\
u(0,t)=\alpha(t)\\
u(l,t)=\beta(t)\\
0<x<l,\ 0\leq t\leq T
\end{cases}, i=1,\ 2,\ \mathrm{L}\ ,\ n,$$

and

$$\begin{cases}
u^i\big|_{x=x^i}=u^{i+1}\big|_{x=x^i}\\
-k^{i+1}\dfrac{\partial u}{\partial x}^{i+1}\Big|_{x=x^i}=-k^i\dfrac{\partial u}{\partial x}^{i}\Big|_{x=x^i}
\end{cases}, 0\leq t\leq T, i=1,\ 2,\ \mathrm{L}\ ,\ n-1,$$

where $c^i(x),\rho^i(x),k^i(x)$ are continuous functions on (x^{i-1},x^i).

Suppose that the temperature distribution at time t_0 has been measured as $u^i(x,t_0)$, while the initial temperature distribution $f(x)$ is an unknown function. We now solve for the temperature function $u(x,t)$.

Reconstructing the temperature function $u^i(x,t)$ only requires solving the initial temperature distribution $f(x)$, similar to the analysis for the forward problem. We can obtain the difference schemes (3.5) and (3.6), and the matrix form (3.7) is as follows:

$$AU_{k+1} = BU_k + C_k,$$

By iteratively applying (3.7) in the time layer $k = 0,1,\mathrm{L}\ ,K-1$, we can obtain

$$U_K = \left(A^{-1}B\right)^K U_0 + \sum_{k=0}^{K-1}\left(A^{-1}B\right)^{K-k-1} A^{-1}C_k\ , \tag{3.31}$$

Note $\left(A^{-1}B\right)^K = T$, $U_K - \sum_{k=0}^{K-1}\left(A^{-1}B\right)^{K-k-1} A^{-1}C_k = F$, then we have

$$TU_0 = F\ . \tag{3.32}$$

The inverse heat conduction problem often has strong ill-posedness, and the Landweber iterative regularization method is a classic method for solving ill-posed problems.

Consider solving the operator equation, namely:

$$Tx = y\,, \tag{3.33}$$

where $x \in X$, $y \in Y$, $T: X \to Y$ is a linear operator on a Banach space. In the solution of the heat conduction inverse problem, the operator equation (3.33) is often an ill-posed problem, meaning that there is no solution, the solution is not unique, or the solution is unstable. It is usually transformed into finding the solution to the least squares problem, namely:

$$x^{\dagger} = \arg\min_{x\in X} \|Tx - y\|_Y^2\,, \tag{3.34}$$

where $\arg\min_{x\in X} f(x)$ is the value of the independent variable x that corresponds to the minimum value of $f(x)$.

For ill-posed problems, the least squares solution is often unstable, and in practical problems, y is often y^{δ} with disturbances, so the least squares solution has a large error from the true solution. This instability is caused by inverting the matrix T, so the Landweber iterative regularization method is used to avoid inverting the matrix T and transform the instability problem into a stable problem.

Proposition 3.4 [25]. If $y \in R(T)$, then $x^{\dagger}$ is a solution to the least squares problem c with the necessary and sufficient condition $T^*Tx^{\dagger} = T^*y$, where T^* is the adjoint operator of T.

To solve the solution of $T^*Tx^{\dagger} = T^*y^{\delta}$, it is first transformed into the following form:

$$\begin{aligned} x^{\dagger} &= x^{\dagger} - \omega\left(T^{*}Tx^{\dagger} - T^{*}y^{\delta}\right) \\ &= \left(I - \omega T^{*}T\right)x^{\dagger} + \omega T^{*}y^{\delta} \end{aligned}, \tag{3.35}$$

where $0 < \omega \le \dfrac{1}{\|T\|^{2}_{L(Y,X)}}$ is the relaxation factor.

Use the fixed-point iteration method to solve for (3.35), as follows:

$$x_0^{\delta} := 0,\ x_m^{\delta} := \left(I - \omega T^{*}T\right)x_{m-1} + \omega T^{*}y^{\delta}, \tag{3.36}$$

where the relaxation factor ω is often taken to be the iteration step size.

Using mathematical induction, we have

$$x_m^{\delta} = \omega\sum_{n=0}^{m-1}\left(I - \omega T^{*}T\right)^{n}T^{*}y^{\delta}. \tag{3.37}$$

By the Banach fixed-point theorem, if $y^{\delta} \notin R(T)$, the iteration will diverge, and data y^{δ} contain noise level δ interference, so the iteration point approaches the true solution at the beginning of the iteration, but the distance between the iteration point and the true solution will increase after a long iteration. Therefore, a stopping criterion must be adopted to stop the iteration at an appropriate time. The Morozov discrepancy principle is often used as it can prevent overfitting of noisy data while maintaining solution stability, effectively approximating the true solution; it only needs to know the noise level compared to a prior criterion.

The Morozov discrepancy principle [26]. For an iterative exponent $m^{*} = m\left(\delta, y^{\delta}\right)$, for given numbers δ, y^{δ}, and a number $\tau \ge 2$ independent of δ, y^{δ}, the iteration will stop when $\left\|Tx_{m^{*}}^{\delta} - y^{\delta}\right\|_{Y} \le \tau\delta \le \left\|Tx_{m^{*}-1}^{\delta} - y^{\delta}\right\|_{Y}$.

We now consider convergence characteristics under the source condition $x^{\dagger} \in X_{v,f}$ for $v, f > 0$.

Theorem 3.5. If $\left\|Tx_m^{\delta} - y^{\delta}\right\|_{Y} > 2\delta$, then $\left\|x_{m+1}^{\delta} - x^{\dagger}\right\|_{X} < \left\|x_m^{\delta} - x^{\dagger}\right\|_{X}$.

Proof. Note $\varphi_m^{\delta} = y^{\delta} - Tx_m^{\delta}$, $y = Tx^{\dagger}$, we have

$$\begin{aligned} \left\|x_{m+1}^{\delta} - x^{\dagger}\right\|_{X}^{2} &= \left\|x_m^{\delta} - x^{\dagger} + \omega T^{*}\varphi_m^{\delta}\right\|_{X}^{2} \\ &= \left\|x_m^{\delta} - x^{\dagger}\right\|_{X}^{2} + 2\omega\left(T\left(x_m^{\delta} - x^{+}\right)\middle|\varphi_m^{\delta}\right)_{Y} + \omega^{2}\left\|T^{*}\varphi_m^{\delta}\right\|_{X}^{2} \\ &= \left\|x_m^{\delta} - x^{\dagger}\right\|_{X}^{2} + \omega\left[\left(y^{\delta} - y\middle|\varphi_m^{\delta}\right)_{Y} + \omega\left\|\varphi_m^{\delta}\right\|_{Y}^{2}\right] + \omega\left(\omega\left\|T^{*}\varphi_m^{\delta}\right\|_{X}^{2} - \left\|\varphi_m^{\delta}\right\|_{Y}^{2}\right) \end{aligned}, \tag{3.38}$$

In particular

$$\omega\left[\left(y^{\delta} - y\middle|\varphi_m^{\delta}\right)_{Y} + \omega\left\|\varphi_m^{\delta}\right\|_{Y}^{2}\right] \le \omega\left(2\delta\left\|\varphi_m^{\delta}\right\|_{Y} - \left\|\varphi_m^{\delta}\right\|_{Y}^{2}\right) = \left(2\delta - \left\|Tx_m^{\delta} - y^{\delta}\right\|_{Y}\right)\left\|\varphi_m^{\delta}\right\|_{Y} < 0, \tag{3.39}$$

and

$$\omega\left\|T^{*}\varphi_m^{\delta}\right\|_{X} - \left\|\varphi_m^{\delta}\right\|_{Y}^{2} \le \omega\left\|T^{*}\right\|_{L(Y,X)}^{2}\left\|\varphi_m^{\delta}\right\|_{Y}^{2} - \left\|\varphi_m^{\delta}\right\|_{Y}^{2} < 0. \tag{3.40}$$

Then we have $\left\|x_{m+1}^{\delta}-x^{\dagger}\right\|_X^2<\left\|x_m^{\delta}-x^{\dagger}\right\|_X^2$, namely $\left\|x_{m+1}^{\delta}-x^{\dagger}\right\|_X<\left\|x_m^{\delta}-x^{\dagger}\right\|_X$.□

Theorem 3.6. The Morozov discrepancy principle terminates the Landweber iteration in step $m^*\le C^*\left(\frac{\|f\|}{\delta}\right)^{\frac{2}{2\nu+1}}$ with some $C>0$.

Proof. Using the Morozov discrepancy principle, we have

$$\tau\delta<\left\|Tx_{m^*-1}^{\delta}-y^{\delta}\right\|_Y=\left\|Tx_{m^*-1}^{\delta}-Tx^{\dagger}+Tx^{\dagger}-y^{\delta}\right\|_Y\le\left\|T\left(x_{m^*-1}^{\delta}-x^{\dagger}\right)\right\|+\delta, \tag{3.41}$$

In particular

$$\begin{aligned}\left\|T\left(x_{m^*-1}^{\delta}-x^{\dagger}\right)\right\|&\le\left\|T\left(x^{\dagger}-x_{m^*-1}\right)\right\|_X+\left\|T\left(x_{m^*-1}^{\delta}-x_{m^*-1}\right)\right\|\\&=\left\|\left(I-\omega T^*T\right)^m T\left(T^*T\right)\right\|_{L(Y,X)}\|f\|+\omega\sum_{i=0}^{m-1}\left\|I-\left(I-\omega T^*T\right)^i\right\|\left\|y^{\delta}-y\right\|,\\&\le\frac{\omega^{-\nu}}{\sqrt{\omega}}\left(m^*\right)^{-\nu-\frac{1}{2}}\|f\|+\delta\end{aligned} \tag{3.42}$$

Hence

$$\omega^{-\nu-\frac{1}{2}}\left(m^*\right)^{-\nu-\frac{1}{2}}\|f\|\ge(\tau-2)\delta, \tag{3.43}$$

This implies that

$$m^*\le C^*\left(\frac{\|f\|}{\delta}\right)^{\frac{2}{2\nu+1}}, \tag{3.44}$$

with some $C^*>0$.□

Theorem 3.7. $\left\|x_m^{\delta}-x^{\dagger}\right\|\le\sqrt{\omega m}\delta+\left(\omega(m+1)\right)^{-\upsilon}$, $\left\|x_{m^*}^{\delta}-x^{\dagger}\right\|\le C\|f\|^{\frac{1}{2\nu+1}}\delta^{\frac{2\nu}{2\nu+1}}$ with some $C>0$.

Proof. Using $x^{\dagger}\in X_{\nu,f}$, we have

$$\left\|x_m^{\delta}-x_m\right\|=\sum_{i=0}^{m-1}\omega\left\|\left(I-\omega T^*T\right)^i T^*\right\|\left\|y^{\delta}-y\right\|\le\sqrt{\omega m}\delta, \tag{3.45}$$

and

$$\left\|x^{\dagger}-x_m\right\|_X=\left\|\left(I-\omega T^*T\right)^m\left(T^*T\right)\right\|_{L(Y,X)}\|f\|\le\left(\omega(m+1)\right)^{-\upsilon}. \tag{3.46}$$

So, we have

$$\left\|x_m^{\delta}-x^{\dagger}\right\|\le\left\|x_m^{\delta}-x_m\right\|+\left\|x^{\dagger}-x_m\right\|\le\sqrt{\omega m}\delta+\left(\omega(m+1)\right)^{-\upsilon} \tag{3.47}$$

By (3.44) and (3.47), we have

$$\left\|x_{m^*}^{\delta}-x^{\dagger}\right\|\le\sqrt{\omega m^*}\delta+\left(\omega\left(m^*+1\right)\right)^{-\upsilon}\le C\|f\|^{\frac{1}{2\nu+1}}\delta^{\frac{2\nu}{2\nu+1}}, \tag{3.48}$$

with some $C>0$.□

4. Numerical examples and discussion

In this section, we shall present some examples to verify our theoretical findings.

4.1. Forward problem

Example 4.1.

$$\begin{cases} \dfrac{\partial u^1}{\partial t}=\dfrac{\partial}{\partial x}\left(\dfrac{\partial u^1}{\partial x}\right),0<x<1 \\ \dfrac{\partial u^2}{\partial t}=\dfrac{\partial}{\partial x}\left(4\dfrac{\partial u^2}{\partial x}\right),1<x<2 \\ u(x,0)=\begin{cases}\sin\left(\dfrac{\pi x}{2}\right),0\le x\le 1\\ \sin\left(\dfrac{\pi(3-x)}{4}\right),1<x\le 2\end{cases} \quad ,0\le t\le 1, \\ u(0,t)=0,u(2,t)=\dfrac{\sqrt{2}e^{-\frac{\pi^2 t}{4}}}{2} \end{cases} \tag{4.1}$$

The exact solution of the equation is as follows:

$$u(x,t)=\begin{cases} e^{-\frac{\pi^2 t}{4}}\sin\left(\dfrac{\pi x}{2}\right),0\le x\le 1 \\ e^{-\frac{\pi^2 t}{4}}\sin\left(\dfrac{\pi(3-x)}{4}\right),1<x\le 2 \end{cases} \quad ,0<t<1. \tag{4.2}$$

Example 4.2.

$$\begin{cases} \dfrac{\partial u^1}{\partial t}=\dfrac{\partial}{\partial x}\left((0.1-0.09x)\dfrac{\partial u^1}{\partial x}\right)+0.09\pi e^{-0.1\pi^2 t}\left(\cos(\pi x)-\pi x\sin(\pi x)\right),0<x<\dfrac{2}{3} \\ \dfrac{\partial u^2}{\partial t}=\dfrac{\partial}{\partial x}\left(0.01\dfrac{\partial u^2}{\partial x}\right)+0.06\pi^2 e^{-0.1\pi^2 t}\sin(4\pi x),\dfrac{2}{3}<x<1 \\ u(x,0)=\begin{cases}\sin(\pi x),0\le x\le\dfrac{2}{3}\\ \sin(4\pi x),\dfrac{2}{3}<x\le 1\end{cases} \quad ,0\le t\le 1, \\ u(0,t)=u(1,t)=0 \end{cases} \tag{4.3}$$

The exact solution of the equation is as follows:

$$u(x,t)=\begin{cases} e^{-0.1\pi^2 t}\sin(\pi x),0\le x\le\dfrac{2}{3} \\ e^{-0.1\pi^2 t}\sin(4\pi x),\dfrac{2}{3}<x\le 1 \end{cases} \quad ,0<t<1. \tag{4.4}$$

Example 4.3.

$$\begin{cases} \dfrac{\partial u^1}{\partial t}=\dfrac{\partial}{\partial x}\left(\dfrac{2-x}{\pi^2}\dfrac{\partial u^1}{\partial x}\right)-(x-1)e^{-t}\sin(\pi x)+\dfrac{1}{\pi}e^{-t}\cos(\pi x), 0<x<1 \\ \dfrac{\partial u^2}{\partial t}=\dfrac{\partial}{\partial x}\left(\dfrac{2}{\pi^2}\dfrac{\partial u^3}{\partial x}\right)-\dfrac{2}{\pi}e^{-t}\cos(\pi x)+\dfrac{1}{2}e^{-t}x\sin(\pi x), 1<x<2 \\ \dfrac{\partial u^3}{\partial t}=\dfrac{\partial}{\partial x}\left(\dfrac{4}{\pi^2}\dfrac{\partial u^3}{\partial x}\right)-\dfrac{2}{\pi}e^{-t}\cos(\pi x)+\dfrac{3}{4}e^{-t}x\sin(\pi x), 2<x<2.5 \\ u(0,t)=0, u(2.5,t)=\dfrac{5}{8} \end{cases}, 0\le t\le 1, \quad (4.5)$$

The exact solution of the equation is as follows:

$$u(x,t)=\begin{cases} e^{-t}\sin(\pi x), 0\le x\le 1 \\ \dfrac{1}{2}e^{-t}x\sin(\pi x), 1<x\le 2 \\ \dfrac{1}{4}e^{-t}x\sin(\pi x), 2<x\le 2.5 \end{cases}, 0\le t\le 1. \quad (4.6)$$

Solve for the temperature function $u(x,t)$. Take $\theta=\dfrac{1}{2}$. Divide the space interval and the time interval into equal parts by the space-step size $h=\dfrac{1}{60}$ and the time-step size $\tau=\dfrac{1}{30}$. Table 1 shows the maximum error under different difference methods. Figure 2 shows the error diagram under the proposed method.

Table 1. Maximum error of different difference methods.

Example	Finite volume method	Harmonic mean	Arithmetic mean
4.1	1.97×10^{-4}	2.03×10^{-4}	2.06×10^{-4}
4.2	1.38×10^{-3}	1.61×10^{-3}	1.83×10^{-3}
4.3	5.97×10^{-5}	6.61×10^{-5}	7.45×10^{-5}

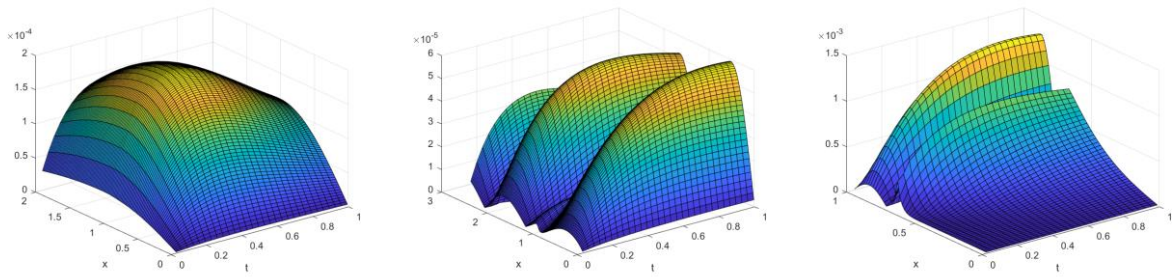

(a) Example 4.1. (b) Example 4.2. (c) Example 4.3.

Figure 2. Error diagram for the forward problem.

4.2. Inverse problem

Example 4.4.

$$\begin{cases} \dfrac{\partial u^1}{\partial t}=\dfrac{\partial}{\partial x}\left(\dfrac{\partial u^1}{\partial x}\right), 0<x<1 \\ \dfrac{\partial u^2}{\partial t}=\dfrac{\partial}{\partial x}\left(4\dfrac{\partial u^2}{\partial x}\right), 1<x<2 \\ u(x,1)=\begin{cases} e^{-\frac{\pi^2}{4}}\sin\left(\dfrac{\pi x}{2}\right), 0\le x\le 1 \\ e^{-\frac{\pi^2}{4}}\sin\left(\dfrac{\pi(3-x)}{4}\right), 1<x\le 2 \end{cases} , 0\le t\le 1 \\ u(0,t)=0, u(2,t)=\dfrac{\sqrt{2}e^{-\frac{\pi^2 t}{4}}}{2} \end{cases} \tag{4.7}$$

The exact solution of the equation is:

$$u(x,t)=\begin{cases} e^{-\frac{\pi^2 t}{4}}\sin\left(\dfrac{\pi x}{2}\right), 0\le x\le 1 \\ e^{-\frac{\pi^2 t}{4}}\sin\left(\dfrac{\pi(3-x)}{4}\right), 1<x\le 2 \end{cases} , 0<t<1. \tag{4.8}$$

Example 4.5.

$$\begin{cases} \dfrac{\partial u^1}{\partial t}=\dfrac{\partial}{\partial x}\left((0.1-0.09x)\dfrac{\partial u^1}{\partial x}\right)+0.09\pi e^{-0.1\pi^2 t}\left(\cos(\pi x)-\pi x\sin(\pi x)\right), 0<x<\dfrac{2}{3} \\ \dfrac{\partial u^2}{\partial t}=\dfrac{1}{\pi}\dfrac{\partial}{\partial x}\left(0.01\dfrac{\partial u^3}{\partial x}\right)+0.06\pi^2 e^{-0.1\pi^2 t}\sin(4\pi x), \dfrac{2}{3}<x<1 \\ u(x,1)=\begin{cases} e^{-0.1\pi^2}\sin(\pi x), 0\le x\le \dfrac{2}{3} \\ e^{-0.1\pi^2}\sin(4\pi x), 1<x\le \dfrac{2}{3} \end{cases} , 0\le t\le 1. \\ u(0,t)=u(1,t)=0 \end{cases} \tag{4.9}$$

The exact solution of the equation is:

$$u(x,t)=\begin{cases} e^{-0.1\pi^2 t}\sin(\pi x),\ 0\le x\le 1 \\ e^{-0.1\pi^2 t}\sin(4\pi x),\ 1<x\le 2 \end{cases} ,\ 0<t<1, \tag{4.10}$$

Example 4.6.

$$\begin{cases} \dfrac{\partial u^1}{\partial t}=\dfrac{\partial}{\partial x}\left(\dfrac{2-x}{\pi^2}\dfrac{\partial u^1}{\partial x}\right)-(x-1)e^{-t}\sin(\pi x)+\dfrac{1}{\pi}e^{-t}\cos(\pi x), 0<x<1 \\ \dfrac{\partial u^2}{\partial t}=\dfrac{\partial}{\partial x}\left(\dfrac{2}{\pi^2}\dfrac{\partial u^3}{\partial x}\right)-\dfrac{2}{\pi}e^{-t}\cos(\pi x)+\dfrac{1}{2}e^{-t}x\sin(\pi x), 1<x<2 \\ \dfrac{\partial u^3}{\partial t}=\dfrac{\partial}{\partial x}\left(\dfrac{4}{\pi^2}\dfrac{\partial u^3}{\partial x}\right)-\dfrac{2}{\pi}e^{-t}\cos(\pi x)+\dfrac{3}{4}e^{-t}x\sin(\pi x), 2<x<2.5 \\ u(x,1)=\begin{cases} e^{-1}\sin(\pi x), 0\le x\le 1 \\ \dfrac{e^{-1}}{2}x\sin(\pi x), 1<x\le 2 \\ \dfrac{e^{-1}}{4}x\sin(\pi x), 2<x\le 2.5 \end{cases} \\ u(0,t)=0, u(2.5,t)=\dfrac{5}{8}e^{-t} \end{cases} , 0\le t\le 1. \tag{4.11}$$

The exact solution of the equation is:

$$u(x,t)=\begin{cases} e^{-t}\sin(\pi x), 0\le x\le 1 \\ \dfrac{e^{-t}}{2}x\sin(\pi x), 1\le x\le 2 \\ \dfrac{e^{-t}}{4}x\sin(\pi x), 2<x\le 2.5 \end{cases} , 0<t<1, \tag{4.12}$$

Consider a perturbation $\delta=0.001\sin(x)$ in the measured value $u(x,1)$. Reconstruct the temperature function $u(x,t)$. Take $\theta=\dfrac{1}{2}$. Divide the space interval and the time interval into equal parts by the space-step size $h=\dfrac{1}{60}$ and the time-step size $\tau=\dfrac{1}{30}$. Table 2 shows the maximum errors under different difference methods. Table 3 shows the maximum errors under different regularization methods. Figure 3 shows the error diagram under the proposed method.

Table 2. Maximum errors of different difference methods.

Example	Finite volume method	Harmonic mean	Arithmetic mean
4.4	0.0117	0.0143	0.0188
4.5	0.0669	0.0789	0.0833
4.6	0.0355	0.0457	0.0521

Table 3. Maximum errors of different regularization methods.

Example	Landweber iteration	Tikhonov regularization	Conjugate gradient
	$\left(\omega = \frac{1}{\|T\|^2}\right)$	$\left(\alpha = 10^{-3}\right)$	$\left(r = 10^{-6}\right)$
4.4	0.0117	0.0224	0.0130
4.5	0.0669	0.0767	0.0675
4.6	0.0355	0.0552	0.0468

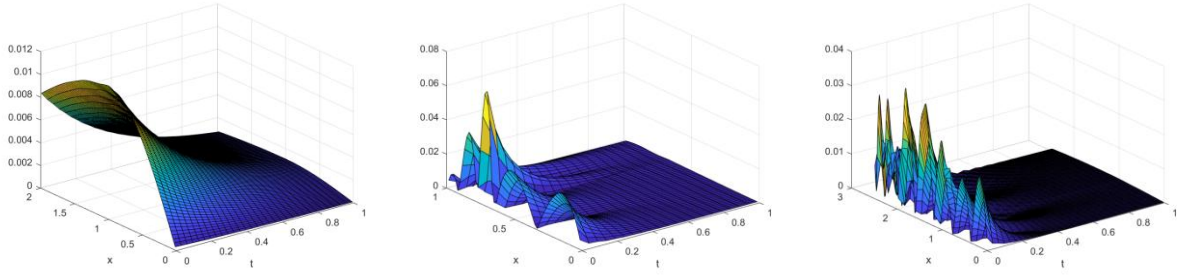

(a) Example 4.4. (b) Example 4.5. (c) Example 4.6.

Figure 3. Error diagram for the inverse problem.

It can be seen from these graphs that the finite volume method is more efficient than traditional difference methods, especially in the inversion of heat conduction in heterogeneous media. In the case of given regularization parameters and tolerances, Landweber iteration is more accurate than the Tikhonov regularization and conjugate gradient methods, but it also takes a longer time for calculation.

As can be observed in Figures 2 and 3, the forward problem and inversion problem show different error evolution patterns. In the forward problem, truncation errors introduce minor inaccuracies during each time step. These inaccuracies progressively accumulate with iterations, manifesting as an error growth pattern. Conversely, for the inverse problem, the diffusion of heat conduction induces progressive smoothing of high-frequency components in initial conditions over time. Early time nodes require recovering high-frequency features from severely attenuated signals, amplifying noise sensitivity and reconstruction errors; later time nodes benefit from reduced signal attenuation, enabling more stable recovery with diminished errors, manifesting as an error decay pattern.

4.3. Sensitivity analysis

Consider Example 4.2. Changing the number of time nodes and space nodes, the maximum error variation under the proposed method is shown in Figure 4.

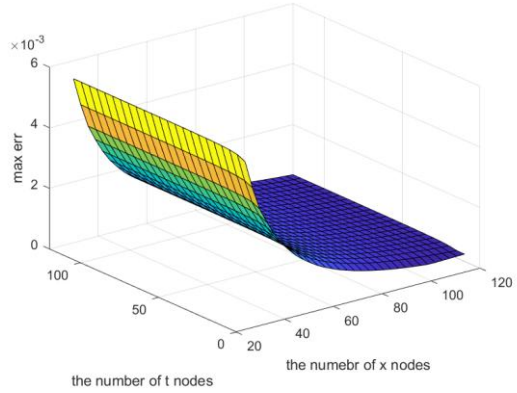

Figure 4. Maximum error variation for Example 4.2.

Consider Example 4.5. Fixing the noise level $\|\delta\|_\infty = 0.001$, and changing the numbers of time nodes and space nodes, the maximum error variation under the proposed method is shown in Figure 5.

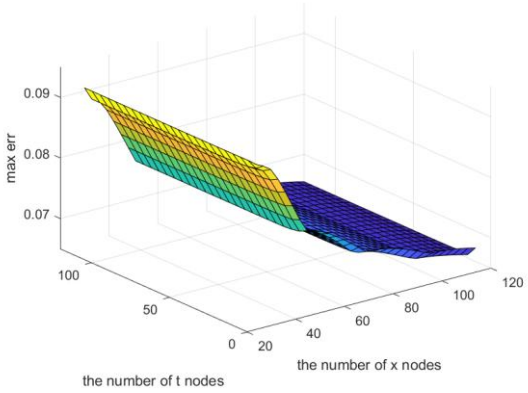

Figure 5. Maximum error variation for Example 4.5.

For fixed time nodes and space nodes, changing the noise level $\|\delta\|_\infty$, the maximum error variation under different regularization methods is shown in Figure 6.

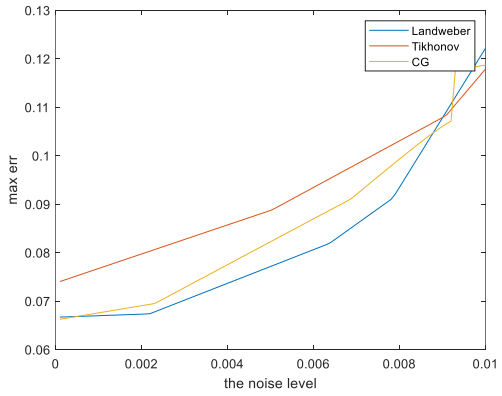

Figure 6. Maximum errors variations at fixed mesh for Example 4.5.

For fixed time nodes and noise level $\|\delta\|_\infty = 0$, setting the maximum number of iterations to 10^6 and changing the number of space nodes, the maximum error variation under the proposed method is shown in Figure 7.

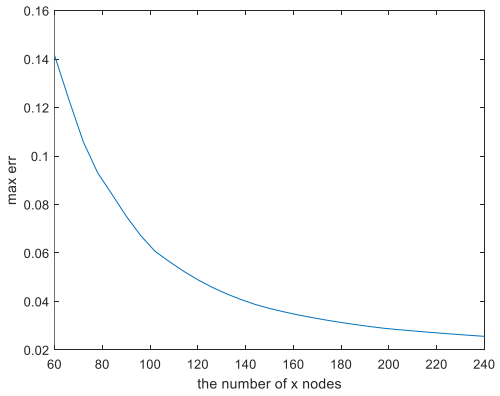

Figure 7. Maximum error variation at $\delta = 0$ for Example 4.5.

As shown in Figures 4 and 5, the error decreases effectively with increasing temporal and spatial node counts. A slower error reduction with temporal nodes occurs because the error is predominantly influenced by space nodes with lower convergence orders. In Figure 5, however, the error declines even more gradually, since increasing nodes only mitigates inherent errors of the difference scheme itself, not additional perturbations caused by external disturbances. Figure 6 demonstrates that the Landweber iteration exhibits stronger noise resistance compared to the Tikhonov and conjugate gradient methods. Notably, residual errors persist even at zero noise levels due to the intrinsic limitations of the difference scheme. Figure 7 reveals that increasing space node counts effectively reduces errors when noise is absent, highlighting the method's theoretical convergence potential under ideal conditions.

5. Conclusions

Heat conduction in multi-layered media presents a persistent research challenge. We constructed a difference scheme using the finite volume method to address the forward problem. To solve the inverse problem, we employed the Landweber iterative regularization method, incorporating the difference scheme developed for the forward problem. We validated the method through numerical experiments, including comparative studies with existing approaches and sensitivity analyses. The proposed method demonstrates enhanced accuracy and effectiveness, showing superior precision and noise resistance compared to conventional methods.

Despite significant progress in heat conduction research for multi-layered media, challenges persist. The finite volume method requires high-precision discretization of accurate solutions, which increases computational costs and reduces the stability of operator equations in inverse problems. To enhance both efficiency and accuracy, adopting more effective approaches like the finite element method for deriving numerical schemes should be considered. While effective in numerical verification, the Landweber iterative regularization we employed suffers from high computational costs and lengthy processing times. In numerical experiments, we found that the Tikhonov regularization and conjugate gradient methods demonstrate superior computational efficiency. These

methods could serve as alternatives to the Landweber iteration method when high precision and stability are not strictly required. Alternatively, improvements can be sought to enhance accuracy while preserving efficiency—such as determining appropriate regularization parameters [27]. Meanwhile, accelerating the Landweber iteration method presents another viable direction for boosting computational speed. Accelerated Landweber iteration could focus on three primary strategies: optimizing the iteration scheme [28], developing effective preconditioning techniques [29], and implementing adaptive weight adjustment strategies [30]. These methods achieved more efficient results than the Tikhonov regularization and conjugate gradient methods. Future research should focus on developing high-accuracy and high-efficiency solution methods.

Author contributions

Yu Xu: conceived the idea and wrote original draft; Youjun Deng: analyzed formulas and proofreading manuscripts; Dong Wei: verified the analytical methods and analyzed the result. All authors have read and approved the final version of the manuscript for publication.

Use of Generative-AI tools declaration

The authors declare they have not used artificial intelligence (AI) tools in the creation of this article.

Acknowledgments

This work of Y. Deng was supported by NSFC-RGC Joint Research Grant No. 12161160314 and State Key Laboratory of Aerodynamics.

Conflict of interest

The authors declare no conflict of interest in this paper.

Youjun Deng is the guest editor of special issue “Inverse problem and its applications in imaging and material science” or AIMS mathematics. Youjun Deng was not involved in the editorial review and the decision to publish this article.

References

1. Udayraj, P. Talukdar, A. Das, R. Alagirusamy, Heat and mass transfer through thermal protective clothing—A review, *Int. J. Therm. Sci.*, **106** (2016), 32–56. https://doi.org/10.1016/j.ijthermalsci.2016.03.006
2. Z. Zhang, Y. Xiong, F Guo, Analysis of wellbore temperature distribution and influencing factors during drilling horizontal wells, *J. Energy Resour. Technol.*, **140** (2018), 092901. https://doi.org/10.1115/1.4039744
3. P. M. Sutheesh, A. Chollackal, Thermal performance of multilayer insulation: A review, In: *IOP conference series: Materials science and engineering*, **396** (2018), 012061. https://doi.org/10.1088/1757-899X/396/1/012061

4. L. Kong, L. Zhu, Y. Deng, H. Liu, Electro-osmotic flow within multi-layer microfluidic structures and an algebraic framework for hydrodynamic cloaking and shielding, *SIAM J. Appl. Math.*, **84** (2024), 2365–2392. https://doi.org/10.1137/24M1674078
5. L. Kong, L. Zhu, Y. Deng, X. Fang, Enlargement of the localized resonant band gap by using multi-layer structures, *J. Comput. Phys.*, **518** (2024), 113308. https://doi.org/10.1016/j.jcp.2024.113308
6. Y. Deng, L. Kong, H. Liu, L. Zhu, Elastostatics within multi-layer metamaterial structures and an algebraic framework for polariton resonances, *ESAIM*, **58** (2024), 1413–1440. https://doi.org/10.1051/m2an/2024041
7. Y. Deng, H. Liu, Y. Wang, Identifying active anomalies in a multi-layered medium by passive measurement in EIT, S*IAM J. Appl. Math.*, **84** (2024), 1362–1384. https://doi.org/10.1137/23M1599458
8. X. Fang, Y. Deng, On plasmon modes in multi-layer structures, *Math. Method. Appl. Sci.*, **46** (2023), 18075–18095. https://doi.org/10.1002/mma.9546
9. T. Liu, C. Zhao, Dynamic analyses of multilayered poroelastic media using the generalized transfer matrix method, *Soil Dyn Earthq Eng*, **48** (2013), 15–24. https://doi.org/10.1016/j.soildyn.2012.12.006
10. L. B. Lesem, F. Greytok, F. Marotta, J. J. McKetta Jr, A method of calculating the distribution of temperature in flowing gas wells, *Trans. AIME*, **210** (1957), 169–176. https://doi.org/10.2118/767-G
11. L. Landweber, An iteration formula for Fredholm integral equations of the first kind, *Am. J. Math.*, **73** (1951), 615–624. https://doi.org/10.2307/2372313
12. A. A. Tikhonov, V. V. Glasko, Methods of determining the surface temperature of a body, *Ussr Comput. Math. Math. Phys.*, **7** (1967), 267–273. https://doi.org/10.1016/0041-5553(67)90161-9
13. L. Elden, Approximations for a Cauchy problem for the heat equation, *Inverse Probl.*, **3** (1987), 263. https://doi.org/10.1088/0266-5611/3/2/009
14. L. Elden, Hyperbolic approximations for a Cauchy problem for the heat equation, *Inverse Probl.*, **4** (1988), 59. https://doi.org/10.1088/0266-5611/4/1/008
15. C. H. Huang, S. P. Wang, A three-dimensional inverse heat conduction problem in estimating surface heat flux by conjugate gradient method, *Int. J. Heat Mass Tran.*, **42** (1999), 3387–3403. https://doi.org/10.1016/S0017-9310(99)00020-4
16. J. M. Connors, J. S. Howell, W. J. Layton, Partitioned time stepping for a parabolic two domain problem, *SIAM J Numer. Anal.*, **47** (2009), 3526–3549. https://doi.org/10.1137/080740891
17. A. Shi, Z. Liu, X. Wang, Finite Analytic numerical method for the fluid flows and heat transfer in heterogeneous media (In Chinese), *Chinese Quarterly of Mechanics*, **40** (2019), 645–655. https://doi.org/10.15959/j.cnki.0254-0053.2019.04.01
18. Y. Wang, Y. Xu, D Xu, J. Fan, Optimization of multilayer clothing assemblies for thermal comfort in cold climate, *Int. J. Therm. Sci.*, **179** (2022), 107586. https://doi.org/10.1016/j.ijthermalsci.2022.107586
19. W. Wu, Y. Yang, H. Zheng, S. Wang, N. Zhang, Y. Wang, Investigation of the effective hydro-mechanical properties of soil-rock mixtures using the multiscale numerical manifold model, *Comput. Geotech.*, **155** (2023), 105191. https://doi.org/10.1016/j.compgeo.2022.105191

20. Y. Yang, W. Wu, H. Zheng, S. Wang, L. Yang, An efficient monolithic multiscale numerical manifold model for fully coupled nonlinear saturated porous media, *Comput. Method. Appl. M.*, **418** (2024), 116479. https://doi.org/10.1016/j.cma.2023.116479
21. Y. Hou, X. Zhang, S. Wang, A stabilized state-based peridynamic heat conduction model for interface thermal resistance problems, *Appl. Math. Model.*, **137** (2025), 115504. https://doi.org/10.1016/j.apm.2024.05.001
22. Y. Hou, X. Zhang, A bond-augmented stabilized method for numerical oscillations in non-ordinary state-based peridynamics, *Eng. Fract. Mech.*, **307** (2024), 110276. https://doi.org/10.1016/j.engfracmech.2024.110276
23. W. Wu, Y. Jiao, F. Zheng, J. Zou, S. Wang, NMM-based computational homogenization for nonlinear transient heat conduction in imperfectly bonded heterogeneous media, *Int. Commun. Heat Mass*, **162** (2025), 108599. https://doi.org/10.1016/j.icheatmasstransfer.2025.108599
24. W. Wu, Y. Yang, Y. Jiao, S. Wang, Stability analysis of unsaturated slopes under rainfall and drainage using the vector-sum-based numerical manifold model, *Comput. Geotech.*, **179** (2025), 106992. https://doi.org/10.1016/j.compgeo.2024.106992
25. M. T. Nair, Regularization of ill-posed operator equations: An overview, *J. Anal.*, **29** (2021), 519–541. https://doi.org/10.1007/s41478-020-00263-9
26. O. Scherzer, The use of Morozov's discrepancy principle for Tikhonov regularization for solving nonlinear ill-posed problems. *Computing*, **51** (1993), 45–60. https://doi.org/10.1007/BF02243828
27. R. Molero, M. Martínez-Pérez, C. Herrero-Martín, J. Reventós-Presmanes, I. Roca-Luque, L. Mont, et al., Improving electrocardiographic imaging solutions: A comprehensive study on regularization parameter selection in L-curve optimization in the Atria. *Comput. Biol. Med.*, **182** (2024), 109141. https://doi.org/10.1016/j.compbiomed.2024.109141
28. L. Chen, Y. Li, F. Shen, R. Xue, General temperature computational method of linear heat conduction multilayer cylinder, *J. Iron Steel Res. Int.*, **17** (2010), 33–37. https://doi.org/10.1016/S1006-706X(10)60041-6
29. S. Xie, G. Qu, W. Li, A preconditioned Landweber iteration-based Bundle adjustment for large-scale 3D reconstruction, *Commun. Nonlinear Sci.*, **130** (2023), 107770. https://doi.org/10.1016/j.cnsns.2023.107770
30. F. de Monte, An analytic approach to the unsteady heat conduction processes in one-dimensional composite media, *Int. J. Heat Mass Tran.*, **45** (2002), 1333–1343. https://doi.org/10.1016/S0017-9310(01)00226-5